Research article

Liping Gong[a], Xiaohe Zhang[a], Bing Gu*, Zhuqing Zhu, Guanghao Rui, Jun He, Qiwen Zhan* and Yiping Cui*

Optical pulling forces on Rayleigh particles using ambient optical nonlinearity

https://doi.org/10.1515/nanoph-2019-0095
Received March 28, 2019; revised May 7, 2019; accepted May 8, 2019

Abstract: Optical pulling forces exerted on small particles can be achieved by tailoring the properties of the electromagnetic field, the particles themselves, or the surrounding environment. However, the nonlinear optical effect of the surrounding environment has been largely neglected. Herein, we report the optical pulling forces on a Rayleigh particle immersed in a nonlinear optical liquid using high-repetition-rate femtosecond laser pulses. The analytic expression of time-averaged optical forces allows us to better understand the underlying mechanism of the particle transportation. It is shown that the two-photon absorption of the surrounding liquid gives rise to a negative radiation force. Transversely confined Rayleigh particles can be continuously dragged towards the light source during a pulling process.

Keywords: pulling force; laser trapping; nonlinear optical effect; two-photon absorption; femtosecond laser pulses.

PACS: 78.20.Bh; 78.67.Bf; 87.80.Cc; 62.65.An; 42.65.Re.

[a]**Liping Gong and Xiaohe Zhang:** These authors contributed equally to this work.
***Corresponding authors: Bing Gu and Yiping Cui,** Advanced Photonics Center, Southeast University, Nanjing 210096, Jiangsu, China, e-mail: gubing@seu.edu.cn (B. Gu). https://orcid.org/0000-0002-7060-6046 (B. Gu); cyp@seu.edu.cn (Y. Cui);
and **Qiwen Zhan,** Department of Electro-Optics and Photonics, University of Dayton, 300 College Park, Dayton, OH 45469-2951, USA; and School of Optical-Electrical and Computer Engineering, University of Shanghai for Science and Technology, Shanghai 200093, China, e-mail: qzhan1@udayton.edu
Liping Gong, Xiaohe Zhang and Guanghao Rui: Advanced Photonics Center, Southeast University, Nanjing 210096, Jiangsu, China
Zhuqing Zhu: Key Laboratory of Optoelectronic Technology of Jiangsu Province, School of Physical Science and Technology, Nanjing Normal University, Nanjing 210023, Jiangsu, China
Jun He: School of Physics and Electronics, Central South University, Changsha 410012, China

1 Introduction

In the past 40 years, an optical tweezers technique has experienced impressive progress for trapping and manipulating small objects in air [1], in vacuum [2, 3], in liquid [4, 5], in solid [6, 7], or at interfaces [8–10], taking advantages of the optical forces produced by a tightly focused continuous-wave laser beam [4, 5]. This technique has become a very important tool in various disciplines, including optics [5], quantum physics [2], biological science [6, 11], and chemistry [12]. Recently, the optical tweezers technique has been extended by substituting a continuous-wave laser with high-repetition-rate femtosecond laser pulses [13–16]. In the femtosecond laser tweezers, the high peak intensity of each laser pulse leads to instantaneous trapping of a particle and the high-repetition-rate ensures repetitive trapping by successive pulses. Interestingly, femtosecond laser pulses have revealed novel phenomena in the optical trapping of particles, such as the trapping split behavior in the process of capturing gold nanoparticles [13], directional ejection of optically trapped nanoparticles [16, 17], and immobilization dynamics of a single polystyrene sphere [15]. Moreover, it has been demonstrated that the nonlinear optical effects originating from the particle could modify the optical trapping potential [13], enable the realization of super-resolution optical manipulation [18], or enhance the optical force [14, 19–21]. It is noteworthy that the optical force arising from nonlinear polarization becomes significant and cannot be neglected if the trapped particles exhibit nonlinear optical effects [13, 18, 21–27]. However, the nonlinear optical response of the surrounding medium has never been considered before.

Theoretically, the optical forces exerted on a particle are divided into two parts: one is the gradient force, which is proportional to the gradient of intensity and drives the particle toward the equilibrium point [5]; the other is the radiation (i.e. scattering and absorption) force, which is proportional to the orbital part of the Poynting vector of the field and destabilizes the trap [28–31]. In general, the radiation force acts as a *pushing* force (i.e. in the direction of a beam's propagation) on a particle. However, the particle can be pulled by the negative radiation (scattering) force towards the light source. Recently, this counterintuitive optical *pulling* force has received great attention due to its academic interest and technological applications [32–48].

The physical mechanisms of this pulling force can be exploited by the optical gradient force [33], backward scattering force [34], and/or negative photophoretic force [35, 36]. Through manipulation of the properties of the electromagnetic field, researchers realized the optical pulling force on particles with super-oscillating beams [37], solenoid beams [38], interference of multiple beams [34], nonparaxial gradientless beams [39], two interfering waves [40], etc. By contrast, the shape and material composition of a small particle have been modified to obtain the pulling force, including gain media [41, 42], microspheres with antireflection coatings [43], and chiral particles [44, 45]. In addition, optical pulling on particles can also be achieved through the use of surrounding media with specifically designed properties, such as resonator-waveguide systems [46], hyperbolic metamaterials [7], photonic crystal waveguides [47], and bilayer PT-symmetric structures [48].

In this work, we report the theoretical investigation of optical pulling forces on a dielectric Rayleigh particle immersed in nonlinear optical liquids (e.g. carbon disulfide) arising from focused femtosecond laser pulses. It is found that the two-photon absorption of the surrounding liquid is the predominant physical mechanism for the negative radiation force.

2 Theory

In the optical trapping experiment using high-repetition-rate femtosecond laser pulses, the pulse duration τ_F (FWHM) and repetition-rate v (i.e. the inverse of the pulse period T) for a commercial Ti:sapphire laser are typically about 100 fs and 80 MHz, respectively [13–16]. Accordingly, the spectral bandwidth is so narrow that the pulsed laser can be regarded as a monochromatic field. Hence, the spatial and temporal characteristics of laser pulses can be treated independently. For laser pulses with a Gaussian temporal envelope, the time-harmonic electromagnetic waves are expressed as:

$$\vec{E}(\vec{r},t)=\vec{E}_0(\vec{r})\exp(-i\omega t)\exp[-2\ln(2)t^2/\tau_F^2], \tag{1}$$

$$\vec{B}(\vec{r},t)=\frac{1}{i\omega}\nabla\times\vec{E}(\vec{r},t), \tag{2}$$

where $\vec{E}_0(\vec{r})$ is the complex function of position in space and ω is the circular frequency.

Now we consider a homogeneous, isotropic, nonmagnetic spherical particle with a radius R and a permittivity ε_0^p illuminated under an extern field $\vec{E}(\vec{r},t)$ propagating in a medium with a permittivity ε_0^m. In addition, we assume that both the particle and the surrounding medium exhibit instantaneous optical nonlinearities with the third-order nonlinear optical susceptibilities of χ_3^p and χ_3^m, respectively. According to the Clausius-Mossotti relation and taking into account the radiative reaction correction [49, 50], we obtain the particle-induced dipole moment arising from the linear and nonlinear polarizations as:

$$\vec{p}(\vec{r},t)=\frac{\alpha_e(\vec{r},t)}{1-i\alpha_e(\vec{r},t)k^3/(6\pi\varepsilon_0)}\vec{E}(\vec{r},t), \tag{3}$$

$$\alpha_e(\vec{r},t)=4\pi\varepsilon_0R^3\frac{\varepsilon_0^p-\varepsilon_0^m+\chi'|\vec{E}(\vec{r},t)|^2}{\varepsilon_0^p+2\varepsilon_0^m+\chi''|\vec{E}(\vec{r},t)|^2}, \tag{4}$$

where $\chi'=\chi_3^p-\chi_3^m$ and $\chi''=\chi_3^p+2\chi_3^m$. λ Is the wavelength, $k=2\pi/\lambda$ is the wavenumber, and ε_0 is the permittivity of free space.

Under the excitation of ultrafast laser pulses, the time-averaged optical force acting on the Rayleigh particle ($R\ll\lambda$) is [51]:

$$\langle\vec{F}\rangle=\frac{1}{4T}\int_{-T/2}^{T/2}[(\vec{p}+\vec{p}^*)\cdot\nabla(\vec{E}+\vec{E}^*)+\left(\frac{\partial\vec{p}}{\partial t}+\frac{\partial\vec{p}^*}{\partial t}\right)\times(\vec{B}+\vec{B}^*)]dt, \tag{5}$$

where * denotes the complex conjugate.

Substituting Eqs. (1)–(4) into Eq. (5) (see Section 1 in Supplementary Information for more details) we get:

$$\langle\vec{F}\rangle=\frac{1}{4}\text{Re}(\alpha)\nabla|\vec{E}_0|^2+\frac{k}{\varepsilon_0c}\text{Im}(\alpha)\langle\vec{S}\rangle_{\text{Orb}}, \tag{6}$$

$$\langle\vec{S}\rangle_{\text{Orb}}=\langle\vec{S}\rangle+\frac{\varepsilon_0c}{2k}\text{Im}[(\vec{E}_0^*\cdot\nabla)\vec{E}_0], \tag{7}$$

$$\langle\vec{S}\rangle=\frac{1}{2\mu_0\omega}\text{Im}[\vec{E}_0\times(\nabla\times\vec{E}_0^*)], \tag{8}$$

$$\alpha=\frac{\sqrt{\pi}\tau_F v}{2\sqrt{\ln 2}}(\gamma_L+\gamma_{NL}), \tag{9}$$

$$\gamma_L = \frac{\alpha_0}{1 - i\alpha_0 k^3 / (6\pi\varepsilon_0)}, \tag{10}$$

$$\alpha_0 = 4\pi\varepsilon_0 R^3 \frac{\varepsilon_0^p / \varepsilon_0^m - 1}{\varepsilon_0^p / \varepsilon_0^m + 2}, \tag{11}$$

$$\gamma_{NL} = \frac{12\pi\varepsilon_0 R^3 (\chi_3^p \varepsilon_0^m - \chi_3^m \varepsilon_0^p)}{[\chi'' - 2ik^3 R^3 \chi' / 3]^2} \sum_{j=2}^{\infty} \frac{(-\eta)^j}{\sqrt{j}} |\vec{E}_0|^{2(j-1)}, \tag{12}$$

$$\eta = \frac{\chi'' - 2ik^3 R^3 \chi' / 3}{(\varepsilon_0^p + 2\varepsilon_0^m) - 2ik^3 R^3 (\varepsilon_0^p - \varepsilon_0^m) / 3}, \tag{13}$$

where c and μ_0 are the speed of light and permeability of light in vacuum, respectively.

Eq. (6), which is the basic result of the present work, gives the total optical forces as a sum of the gradient force and the radiation force on a nonlinear optical Rayleigh particle immersed in a nonlinear optical medium. Especially, Eq. (6) degenerates into the ones reported previously [21, 28, 30] for a Rayleigh particle without/with optical nonlinearity when the optical nonlinear response of the surrounding medium is neglected (i.e. $\chi_3^m = 0$). Different from the conventional optical forces originating from the interaction of optical fields with linear polarizations, the optical forces of nonlinear optical particles immersed in a nonlinear optical medium arises from both the linear and nonlinear polarizations. As described by Eq. (6), the optical forces on the nonlinear particle immersed in a nonlinear optical medium strongly depend on the linear and nonlinear optical properties of both the particle and surrounding medium, the distribution of the electric field, and the laser characteristics.

To trap and manipulate nanoparticles, an x-polarized Gaussian beam is focused by a high numerical-aperture (NA) objective lens (see Section 2 in Supplementary Information for more details). It is noteworthy that one determines $\langle \vec{S} \rangle_{\text{orb}} = \langle \vec{S} \rangle$ along the direction of the beam's propagation from Eq. (7) when the input beam is a linearly polarized beam [21]. Hence, the radiation force expressed by Eq. (6) is only proportional to the Poynting vector $\langle \vec{S} \rangle$ in the following analysis. From Eq. (6), it can be seen that the gradient force is mainly determined by the real part of polarizability Re(α), while the radiation force relies on the imaginary part of polarizability Im(α).

For the absorptive particle [i.e. Im(α) > 0] with a refractive index larger than the surrounding medium [i.e. Re(α) > 0], the backward gradient force can be larger or smaller than the positive radiation force, making it easy to realize the trapping or pushing of a high-refractive-index particle, respectively [5]. Interestingly, in order to produce a pulling force on the particle predominantly contributed by the negative radiation force [see Eq. (6)], the necessary requirement of Im(α) < 0 should be satisfied. One could get Im(α) < 0 for the gain particle immersed in a lossless surrounding medium [41, 42]. Alternatively, the negative radiation force can be realized for the particle immersed in a medium with nonlinear absorption, as we will demonstrate below.

3 Numerical simulations and discussions

First, we assume a silicon nitride (Si_3N_4) particle with the size of $R = 40$ nm immersed in carbon disulfide (CS_2). CS_2 is chosen as a solvent because it is readily available. Moreover, it is well documented that CS_2 exhibits a large refractive nonlinearity in the visible region and strong two-photon absorption in the short wavelength region. In addition, both CS_2 and Si_3N_4 are highly transparent in the visible region. Accordingly, the linear absorption of the solution could be safety omitted. The linear and nonlinear optical parameters of both CS_2 and Si_3N_4 within a wavelength range from 400 nm to 650 nm are taken from the reported ones (see Section 3 in Supplementary Information for more details).

Without loss of generality, we take the following parameters unless otherwise mentioned as NA = 0.8, $\tau_F = 100$ fs, $v = 80$ MHz, and the average power of laser pulses $P = 100$ mW for numerical simulations. The optical forces on the Si_3N_4 nanoparticle immersed in CS_2 solvent using tightly focused laser pulses are calculated with Eq. (6) and shown in Figure 1. Figure 1A illustrates the distributions of the longitudinal forces F_z on the particles produced by focused laser pulses on the z-axis ($x = y = 0$) at different wavelengths from 400 nm to 650 nm. Here, positive (or negative) longitudinal forces mean that their direction is along the $+z$ (or $-z$) direction. Obviously, the longitudinal forces exerted on the particle have different behaviors at different wavelengths. Within a wavelength range from 460 nm to 650 nm, the particle can be trapped at the focal plane due to the existence of the mechanical equilibrium point (e.g. Figure 1B1 and B2). However, in a short wavelength region (i.e. 400–460 nm), the particle will be pulled axially towards the light source owing to the strong negative longitudinal force. For an example, as shown in Figure 1B3, the longitudinal trapping force on the particle at 420 nm remains continuously negative during the pulling process. For the transverse force profiles, as shown in Figure 1C, the maximal y-axis force $F_y^{\max}$

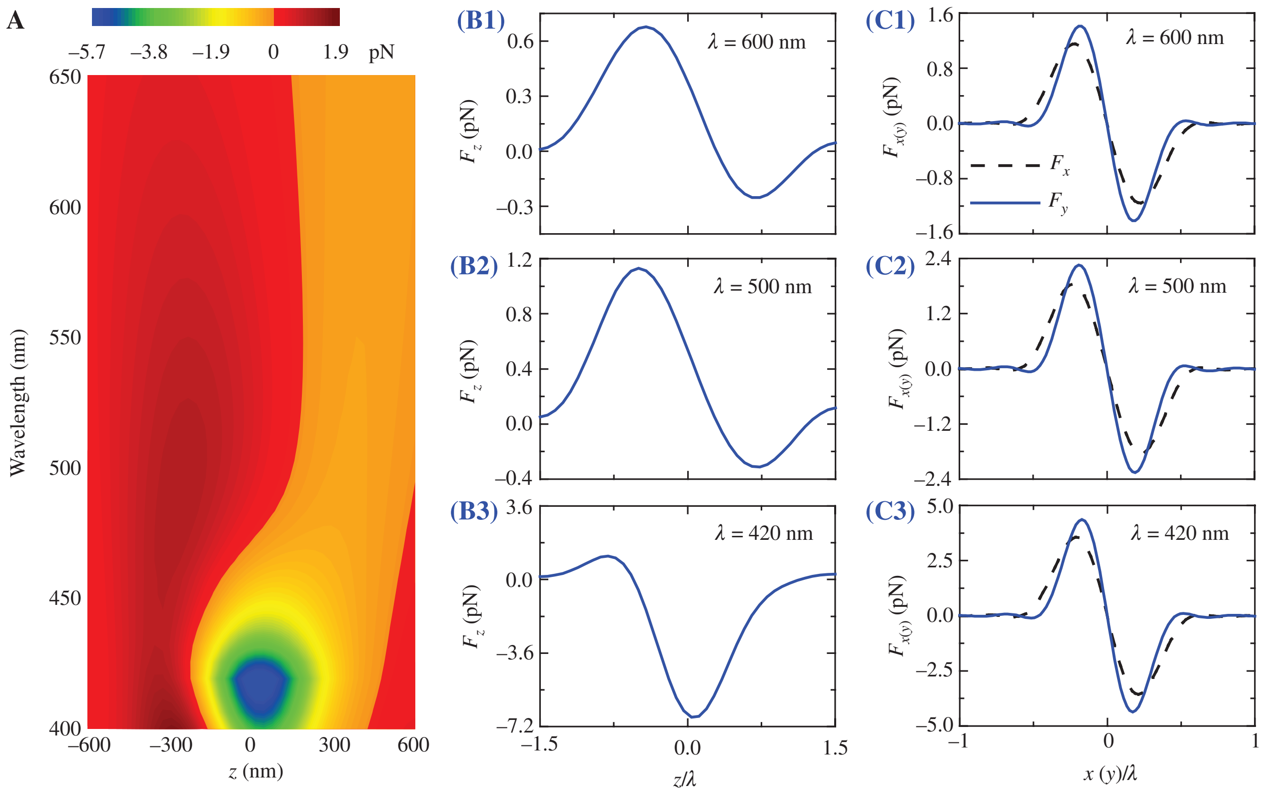

Figure 1: The force distributions produced by tightly focused laser pulses for the Si_3N_4 nanoparticle immersed in CS_2 within a wavelength range from 400 nm to 650 nm.
(A) Longitudinal force on the z-axis ($x=y=0$). (B1)–(B3) The longitudinal force profiles on the z-axis ($x=y=0$) and (C1)–(C3) transverse force profiles in the focal plane ($z=0$) at the wavelengths of 600 nm, 500 nm, and 420 nm.

is obviously larger than F_x^{max}. This is due to the fact that, for the Rayleigh particle, the transverse force is proportional to the intensity gradient of the focused beam. For the x-linearly polarized beam, the intensity gradient along the y-axis appears greater than that in the x-axis. Interestingly, at a wavelength of 420 nm, the Rayleigh particle that is stably trapped in the transverse plane will be continuously pulled towards the light source during the during the 1.5 λ range pulling process (see Section 4 in Supplementary Information for more details).

To gain insight into the physical mechanisms for the pulling force of a nonlinear optical particle immersed in a nonlinear optical medium, we simulate the longitudinal force profiles on the z-axis and transverse force profiles on the y-axis for both the particle and solvent with or without optical nonlinearities at 420 nm. For the solvent without optical nonlinearity (i.e. $\chi_3^m=0$), as shown by the dotted line in Figure 2A, the positive longitudinal force destabilizes the trap by pushing the particle away from the focal plane. When the optical nonlinear effect of the solvent is

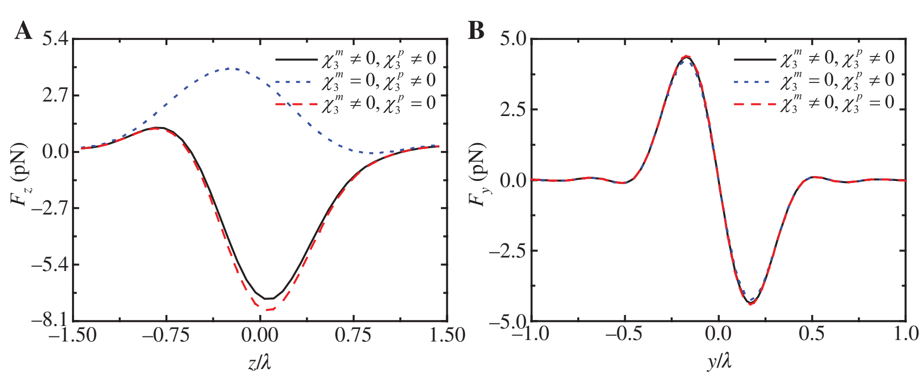

Figure 2: The force profiles for both the particle and solvent with and/or without optical nonlinearities at 420 nm.
(A) The longitudinal force profiles on the z-axis ($x=y=0$) and (B) transverse force profiles on the y-axis ($x=z=0$).

considered (see the solid line in Figure 2A), however, the particle will be pulled towards the light source owing to the negative longitudinal force. For the sake of comparison, the results of the particle without optical nonlinearity (i.e. $\chi_3^p = 0$) are also presented by the dashed line in Figure 2. It is shown that the pulling force still exists whether the particle exhibits the optical nonlinearity or not. Furthermore, the effect of the particle with optical nonlinearity on the pulling force is relatively weak compared with that of the solvent. On the contrary, as shown in Figure 2B, the transverse forces are nearly identical, whether the particle and the solvent have optical nonlinearities or not. It is also noted that the two-photon absorption is a dominant process in the optical nonlinearity of the CS_2 solvent at 420 nm (see Figure S3A in Supplementary Information). Thus, we conclude that the optical pulling forces on the Rayleigh particle are mainly contributed by the radiation forces originating from the two-photon absorption of the surrounding liquid.

Since the power of the laser pulses plays an important role in the nonlinear optical effect and subsequently the optical force, we present in Figure 3A the power dependence of the longitudinal force at the focal point $F_z(r=0)$ and transverse force $F_y^{\max}$ normalized by the power P at 420 nm. It is shown that the value of $F_z(r=0)/P$ becomes increasingly negative as the incident power increases owing to the two-photon absorption of CS_2. At a relatively low power, $F_z(r=0)$ is positive, acting as the pushing force because of the relatively weak nonlinear optical effect. However, when the incident power increases beyond 25 mW, F_z becomes negative and pulls the trapped particle. By contrast, the value of $F_y^{\max} / P$ slowly increases with increasing power. As described by Eq. (6), for the prescribed light field and the excitation wavelength, the radiation force and the gradient force are determined by $\mathrm{Im}(\alpha)$ and $\mathrm{Re}(\alpha)$, respectively. At the focal plane of the focused beam, the values of $\mathrm{Im}(\alpha)$ and $\mathrm{Re}(\alpha)$ are directly related to the longitudinal trapping force and the transverse trapping force, respectively. The values of $\mathrm{Im}(\alpha)$ and $\mathrm{Re}(\alpha)$ as functions of P are shown in Figure 3B as expected. As described by Eq. (9), the polarizability arises from the contributions of both the linear and nonlinear parts. The linear polarizability is independent of P [see Eq. (10)]. However, the nonlinear polarizability depends on the incident optical power [see Eq. (12)]. The imaginary part of the polarizability [i.e. $\mathrm{Im}(\alpha)$] is directly related to the relative absorption coefficient of the particle and the ambient. Due to the relatively strong nonlinear absorption of the ambient, as shown in Figure 3B, the value of $\mathrm{Im}(\alpha)$ decreases approximately linearly with increasing power. On the contrary, the real part of the polarizability [i.e. $\mathrm{Re}(\alpha)$] depends on the relative refraction index of the particle and the ambient. The value of $\mathrm{Re}(\alpha)$ slowly increases as the incident power increases, because of the weak nonlinear refraction effect. It should be emphasized that the value of $\mathrm{Im}(\alpha)$ becomes negative at a relatively high power, resulting in the pulling force on the particle. To enhance the pulling force, one should decrease the negative value of $\mathrm{Im}(\alpha)$. This can be done by increasing either the two-photon absorption of the surrounding medium or the saturable absorption (equivalent to the nonlinear gain) of the particle.

The Si_3N_4 particle in CS_2 is just used as one example of many possible combinations for producing the optical pulling force. To pull the Rayleigh particle confined transversely, there are two necessary requirements to be satisfied: (i) the particle must be stably captured in the transverse plane, i.e. $\mathrm{Re}(\alpha) > 0$; and (ii) the radiation force is negative and directs to the light source, i.e. $\mathrm{Im}(\alpha) < 0$. For the sake of simplicity, we consider the Rayleigh particle with the effective permittivity of $\varepsilon_p^{\mathrm{eff}} = \varepsilon_0^p + \chi_3^p |E|^2$ in CS_2 solvent at 420 nm. Figure 4 illustrates the distributions of the polarizability as a function of real and imaginary parts of the particle's permittivity [i.e. $\mathrm{Re}(\varepsilon_p^{\mathrm{eff}})$ and $\mathrm{Im}(\varepsilon_p^{\mathrm{eff}})$].

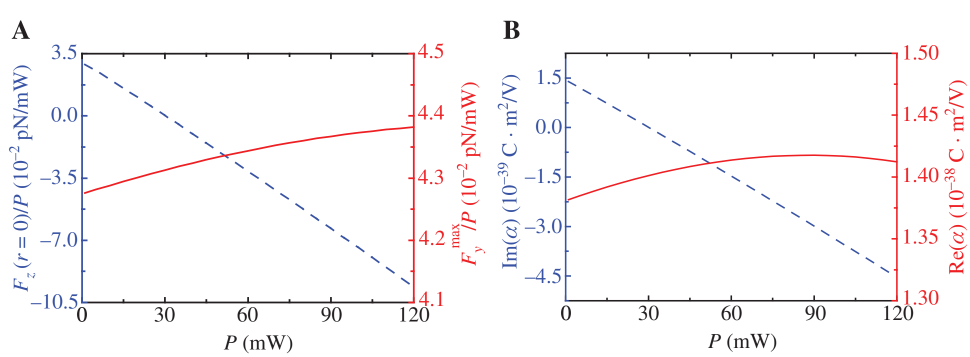

Figure 3: The incident power dependence of (A) the trapping forces and (B) the polarizability α at 420 nm.

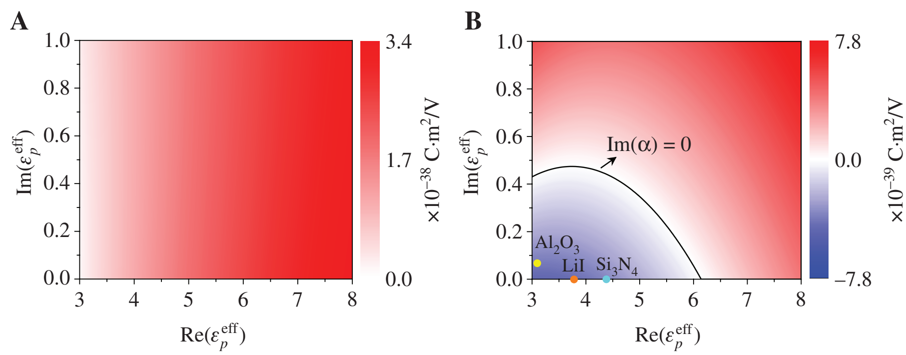

Figure 4: The distributions of (A) Re(α) and (B) Im(α) as a function of real and imaginary parts of a particle's permittivity. The black line in (B) corresponds to the condition of Im(α) = 0. The circle indicates the actual nanoparticles.

As shown in Figure 4A, the value of Re(α), which is nearly independent of Im($\varepsilon_p^{\text{eff}}$), increases as Re($\varepsilon_p^{\text{eff}}$) increases, resulting in the enhancement of the transversely trapping ability. It is found that the condition of Re($\varepsilon_p^{\text{eff}}$) > 3 satisfies the requirement of Re(α) > 0. The distribution of Im(α) as a function of both Re($\varepsilon_p^{\text{eff}}$) and Im($\varepsilon_p^{\text{eff}}$) is shown in Figure 4B. Clearly, both the magnitude and the sign of Im(α) strongly depend on the values of Re($\varepsilon_p^{\text{eff}}$) and Im($\varepsilon_p^{\text{eff}}$). The black line in Figure 4B corresponds the condition of Im(α) = 0. For a high-refractive-index particle with relatively strong absorption, namely, large values of both Re($\varepsilon_p^{\text{eff}}$) and Im($\varepsilon_p^{\text{eff}}$), one obtains the positive value of Im(α). In this case, the radiation force is positive and destabilizes the trap. Interestingly, for particles with a relatively weak absorption, as shown in the bottom-left of Figure 4B, the value of Im(α) is negative. As a result, the radiation force is negative. When the negative radiation force provides a sufficient magnitude against the gradient force, the nanoparticle will be pulled towards the light source. According to this, many nanoparticles such as LiI and Al_2O_3 can generate the optical pulling force in the CS_2 solvent at 420 nm. Thus there is a wide range of particles that can be chosen to utilize this traction behavior.

In addition, we also investigate the influence of the solvent's permittivity on the polarizability of Si_3N_4 nanoparticles at 420 nm. As mentioned above, for the fixed particle, the linear refraction index [i.e. Re(ε_0^m)] and nonlinear absorption coefficient α_2^m of the solvent mainly determine the polarizability. Figure 5 illustrates the distributions of the polarizability as a function of both Re(ε_0^m) and α_2^m. Similar to results in Figure 4, it is found that the value of Re(α), which is nearly independent of α_2^m, decreases as the value of Re(ε_0^m) increases. For the solvent with a high refractive index and large nonlinear absorption coefficient, interestingly, the value of Im(α) is negative as shown in the top-right of Figure 5B. The results suggest that the solvent with a strong nonlinear absorption effect (e.g. CS_2) could provide the optical pulling force on Si_3N_4 nanoparticles at 420 nm.

4 Conclusions

In summary, we studied the time-averaged optical forces exerted on a Rayleigh particle immersed in nonlinear optical solvent using high-repetition-rate ultrafast laser

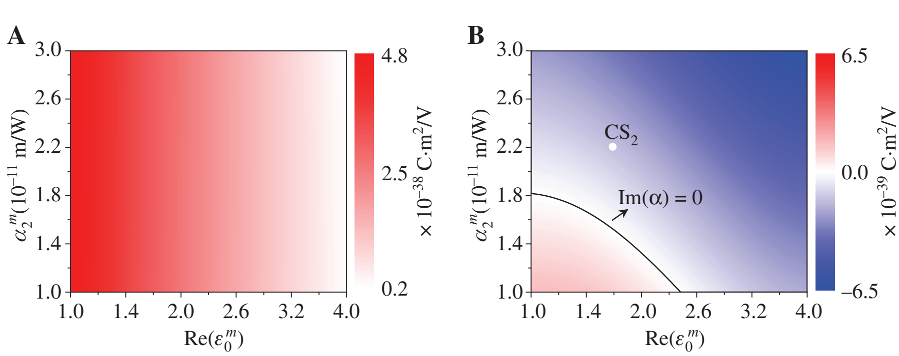

Figure 5: The distributions of (A) Re(α) and (B) Im(α) as a function of Re(ε_0^m) and nonlinear absorption coefficient α_2^m of the solvent. The black line in (B) corresponds to the condition of Im(α) = 0. The circle indicates the actual solvent.

pulses. As an example, we investigated the characteristics of the three-dimensional optical forces for Si_3N_4 nanoparticles immersed in CS_2 at different excitation wavelengths. Interestingly, it is shown that the Rayleigh particle confined transversely can be continuously pulled towards the light source during the pulling process at a specific wavelength (in this study 420 nm). The physical mechanism of the pulling forces is predominantly the negative radiation force originating from the two-photon absorption of the ambient liquid. Beyond the linear optics regime, the concept and results presented in this work provide a novel and practically nonlinear optical approach to manipulate optical forces, resulting in the particle transportation towards the light source.

Acknowledgments: This work was financially supported by the National Science Foundation of China (Funder Id: http://dx.doi.org/10.13039/501100001809, Grant Nos: 11774055, 11474052, and 11504049), Natural Science Foundation of Jiangsu Province (Funder Id: http://dx.doi.org/10.13039/501100004608, BK20171364), and National Key Basic Research Program of China (2015CB352002).

References

[1] Omori R, Kobayashi T, Suzuki A. Observation of a single-beam gradient-force optical trap for dielectric particles in air. Opt Lett 1997;22:816–8.
[2] Li T, Kheifets S, Raizen MG. Millikelvin cooling of an optically trapped microsphere in vacuum. Nat Phys 2011;7:527–30.
[3] Zhou LM, Xiao KW, Chen J, Zhao N. Optical levitation of nanodiamonds by doughnut beams in vacuum. Laser Photon Rev 2017;11:1600284.
[4] Ashkin A. Acceleration and trapping of particles by radiation pressure. Phys Rev Lett 1970;24:156–9.
[5] Ashkin A, Dziedic JM, Bjorkholm JW, Chu S. Observation of a single-beam gradient force optical trap for dielectric particles. Opt Lett 1986;11:288–90.
[6] Keyser UF, Koeleman BN, Van Dorp S, et al. Direct force measurements on DNA in a solid-state nanopore. Nat Phys 2006;2:473–7.
[7] Shalin AS, Sukhov SV, Bogdanov AA, Belov PA, Ginzburg P. Optical pulling forces in hyperbolic metamaterials. Phys Rev A 2015;91:063830.
[8] Dasgupta R, Ahlawat S, Gupta PK. Trapping of micron-sized objects at a liquid-air interface. J Opt A: Pure Appl Opt 2007;9:S189–95.
[9] Park BJ, Furst EM. Optical trapping forces for colloids at the oil-water interface. Langmuir 2008;24:13383–92.
[10] Kajorndejnukul V, Ding W, Sukhov S, Qiu CW, Dogariu A. Linear momentum increase and negative optical forces at dielectric interface. Nat Photonics 2013;7:787–90.
[11] Fazal FM, Block SM. Optical tweezers study life under tension. Nat Photonics 2011;5:318–21.
[12] Ni W, Ba H, Lutich AA, Jäckel F, Feldmann J. Enhancing single-nanoparticle surface-chemistry by plasmonic overheating in an optical trap. Nano Lett 2012;12:4647–50.
[13] Jiang Y, Narushima T, Okamoto H. Nonlinear optical effects in trapping nanoparticles with femtosecond pulses. Nat Phys 2010;6:1005–9.
[14] Chiang WY, Okuhata T, Usman A, Tamai N, Masuhara H. Efficient optical trapping of CdTe quantum dots by femtosecond laser pulses. J Phys Chem B 2014;118:14010–6.
[15] Liu TH, Chiang WY, Usman A, Masuhara H. Optical trapping dynamics of a single polystyrene sphere: continuous wave versus femtosecond lasers. J Phys Chem C 2016;120:2392–9.
[16] Chiang WY, Usman A, Sugiyama T, Hofkens J, Masuhara H. Femtosecond laser trapping dynamics of nanoparticles: a single transient assembly formation leading to their directional ejection. J Phys Chem C 2018;122:13233–42.
[17] Chiang WY, Usman A, Masuhara H. Femtosecond pulse-width dependent trapping and directional ejection dynamics of dielectric nanoparticles. J Phys Chem C 2013;117:19182–8.
[18] Hoshina M, Yokoshi N, Okamoto H, Ishihara H. Super-resolution trapping: a nanoparticle manipulation using nonlinear optical response. ACS Photonics 2018;5:318–23.
[19] Gu M, Bao H, Gan X, Stokes N, Wu J. Tweezing and manipulating micro- and nanoparticles by optical nonlinear endoscopy. Light: Sci Appl 2014;3:e126.
[20] Kittiravechote A, Usman A, Masuhara H, Liau I. Enhanced optical confinement of dielectric nanoparticles by two-photon resonance transition. RSC Adv 2017;7:42606–13.
[21] Gong L, Gu B, Rui G, Cui Y, Zhu Z, Zhan Q. Optical forces of focused femtosecond laser pulses on nonlinear optical Rayleigh particles. Photon Res 2018;6:138–43.
[22] Pobre R, Saloma C. Radiation force on a nonlinear microsphere by a tightly focused Gaussian beam. Appl Opt 2002;41:7694–701.
[23] Kudo T, Ishihara H. Proposed nonlinear resonance laser technique for manipulating nanoparticles. Phys Rev Lett 2012;109:087402.
[24] Kudo T, Ishihara H. Resonance optical manipulation of nano-objects based on nonlinear optical response. Phys Chem Chem Phys 2013;15:14595–610.
[25] Devi A, De AK. Theoretical investigation on nonlinear optical effects in laser trapping of dielectric nanoparticles with ultrafast pulsed excitation. Opt Express 2016;24:21485–96.
[26] Devi A, De AK. Theoretical estimation of nonlinear optical force on dielectric spherical particles of arbitrary size under femtosecond pulsed excitation. Phys Rev A 2017;96:023856.
[27] Zhang Y, Shen J, Min C, et al. Nonlinearity-induced multiplexed optical trapping and manipulation with femtosecond vector beams. Nano Lett 2018;18:5538–43.
[28] Albaladejo S, Marqués MI, Laroche M, Sáenz JJ. Scattering forces from the curl of the spin angular momentum of a light field. Phys Rev Lett 2009;102:113602.
[29] Ruffner DB, Grier DG. Comment on 'scattering forces from the curl of the spin angular momentum of a light field'. Phys Rev Lett 2013;111:059301.
[30] Canaguier-Durand A, Cuche A, Genet C, Ebbesen TW. Force and torque on an electric dipole by spinning light fields. Phy Rev A 2013;88:033831.
[31] Marqués MI. Beam configuration proposal to verify that scattering forces come from the orbital part of the Poynting vector. Opt Lett 2014;39:5122–5.

[32] Brzobohatý O, Karásek V, Šiler M, Chvátal L, Cižmár T, Zemánek P. Experimental demonstration of optical transport, sorting and self-arrangement using a 'tractor beam'. Nat Photonics 2013;7:123–7.
[33] Zhu T, Cao Y, Wang L, et al. Self-induced backaction optical pulling force. Phys Rev Lett 2018;120:123901.
[34] Chen J, Ng J, Lin Z, Chan CT. Optical pulling force. Nat Photonics 2011;5:531–4.
[35] Lin J, Hart AG, Li YQ. Optical pulling of airborne absorbing particles and smut spores over a meter-scale distance with negative photophoretic force. Appl Phys Lett 2015;106:171906.
[36] Lu J, Yang H, Zhou L, et al. Light-induced pulling and pushing by the synergic effect of optical force and photophoretic force. Phys Rev Lett 2017;118:043601.
[37] Sukhov S, Dogariu A. On the concept of 'tractor beams'. Opt Lett 2010;35:3847–9.
[38] Lee SH, Roichman Y, Grier DG. Optical solenoid beams. Opt Express 2010;18:6988–93.
[39] Novitsky A, Qiu C-W, Wang H. Single gradientless light beam drags particles as tractor beams. Phys Rev Lett 2011;107:203601.
[40] Liu H, Panmal M, Peng Y, Lan S. Optical pulling and pushing forces exerted on silicon nanospheres with strong coherent interaction between electric and magnetic resonances. Opt Express 2017;25:12357–71.
[41] Mizrahi A, Fainman Y. Negative radiation pressure on gain medium structures. Opt Lett 2010;35:3405–7.
[42] Webb KJ, Shivanand S. Negative electromagnetic plane-wave force in gain media. Phys Rev E 2011;84:057602.
[43] Jannasch A, Demirörs AF, van Oostrum PDJ, van Blaaderen A, Schäffer E. Nanonewton optical force trap employing anti-reflection coated, high-refractive-index titania microspheres. Nat Photonics 2012;6:469–73.
[44] Ding K, Ng J, Zhou L, Chan CT. Realization of optical pulling forces using chirality. Phys Rev A 2014;89:063825.
[45] Canaguier-Durand A, Genet C. Chiral route to pulling optical forces and left-handed optical torques. Phys Rev A 2015;92:043823.
[46] Intaraprasonk V, Fan S. Optical pulling force and conveyor belt effect in resonator-waveguide system. Opt Lett 2013;38:3264–7.
[47] Zhu T, Novitsky A, Cao Y, et al. Mode conversion enables optical pulling force in photonic crystal waveguides. Appl Phys Lett 2017;111:061105.
[48] Alaee R, Christensen J, Kadic M. Optical pulling and pushing forces in bilayer PT-symmetric structures. Phys Rev Appl 2018;9:014007.
[49] Draine BT. The discrete-dipole approximation and its application to interstellar graphite grains. Astrophys J 1988;333:848–72.
[50] Nieto-Vesperinas M, Sáenz JJ, Gómez-Medina R, Chantada L. Optical forces on small magnetodielectric particles. Opt Express 2010;18:11428–3.
[51] Chaumet P, Nieto-Vesperinas M. Time-averaged total force on a dipolar sphere in an electromagnetic field. Opt Lett 2000;25:1065–7.

Supplementary Material: The online version of this article offers supplementary material (https://doi.org/10.1515/nanoph-2019-0095).